Traffic 2009; **10:** 868–882

doi: 10.1111/j.1600-0854.2009.00919.x

Glycosphingolipid Requirements for Endosome-to-Golgi Transport of Shiga Toxin

Hilde Raa[1,2,3], Stine Grimmer[2], Dominik Schwudke[4], Jonas Bergan[1,2,3], Sébastien Wälchli[2], Tore Skotland[5], Andrej Shevchenko[4] and Kirsten Sandvig[1,2,3,*]

[1] *Centre for Cancer Biomedicine, Faculty Division Norwegian Radium Hospital, University of Oslo, 0316 Oslo, Norway*
[2] *Department of Biochemistry, Institute for Cancer Research, Norwegian Radium Hospital, Rikshospitalet University Hospital, Montebello, 0310 Oslo, Norway*
[3] *Department of Molecular Biosciences, University of Oslo, 0316 Oslo, Norway*
[4] *Max Planck Institute of Molecular Cell Biology and Genetics, 01307 Dresden, Germany*
[5] *GE Healthcare, 0401 Oslo, Norway*
**Corresponding author: Kirsten Sandvig, ksandvig@radium.uio.no*

Received 21 October 2008, revised and accepted for publication 30 March 2009, published online 7 May 2009

Shiga toxin binds to globotriaosylceramide (Gb3) receptors on the target cell surface. To enter the cytosol, Shiga toxin is dependent on endocytic uptake, retrograde transport to the Golgi apparatus and further to the endoplasmic reticulum before translocation of the enzymatically active moiety to the cytosol. Here, we have investigated the importance of newly synthesized glycosphingolipids for the uptake and intracellular transport of Shiga toxin in HEp-2 cells. Inhibition of glycosphingolipid synthesis by treatment with either PDMP or Fumonisin B_1 for 24–48 h strongly reduced the transport of Gb3-bound Shiga toxin from endosomes to the Golgi apparatus. This was associated with a change in localization of sorting nexins 1 and 2, and accompanied by a protection against the toxin. In contrast, there was no effect on transport or toxicity of the plant toxin ricin. High-resolution mass spectrometry revealed a 2-fold reduction in Gb3 at conditions giving a 10-fold inhibition of Shiga toxin transport to the Golgi. Furthermore, mass spectrometry showed that the treatment with PDMP (DL-threo-1-phenyl-2-decanoylamino-3-morpholino-1-propanol) and Fumonisin B_1 among other changes of the lipidome, affected the relative content of the different glycosphingolipid species. The largest depletion was observed for the hexosylceramide species with the *N*-amidated fatty acid 16:0, whereas hexosylceramide species with 24:1 were less affected. Quantitative lipid profiling with mass spectrometry demonstrated that PDMP did not influence the content of sphingomyelins, phospholipids and plasmalogens. In contrast, Fumonisin B_1 affected the amount and composition of sphingomyelin and glycolipids and altered the profiles of phospholipids and plasmalogens.

Key words: Shiga, Golgi, Gb3, glycosphingolipids, endosome, retromer

Shiga toxin is a potent ribosome-inactivating protein produced and secreted by *Shigella dysenteriae*. To reach the ribosomes, the toxin is dependent on endocytic uptake and retrograde transport via the Golgi apparatus to the endoplasmic reticulum (ER) from where it is translocated to the cytosol (1). The toxin consists of two moieties, A and B. The A-chain is the actual toxin, an rRNA specific *N*-glycosidase (2) that cleaves the 28 sRNA of the large ribosomal subunit at a specific site in an exposed loop, rendering elongation factors unable to bind to the ribosome, thus inhibiting protein synthesis. The B-moiety is responsible for binding and needed for uptake and retrograde transport of the toxin (3–5) and it is therefore the crucial entity for cell entry. On the plasma membrane, it specifically recognizes and binds its receptor, the glycosphingolipid globotriaosylceramide (Gb3), Gal(α1 – 4)Gal(β1 – 4)GlcCer. Each B-moiety is a homopentamer which can bind 10–15 molecules of Gb3 (3). Binding of Shiga toxin to its receptor has been suggested to induce recruitment of the toxin/receptor complex to membrane microdomains in the plasma membrane (6), it has been reported to induce tubule formation in the plasma membrane (7), and there is a subsequent internalization which can occur both by clathrin-dependent and clathrin-independent endocytosis (7–10). Importantly, the A-moiety of the toxin can affect the pathway used (10). After internalization, the Shiga toxin/Gb3 complex has, like other glycosphingolipid-bound toxins, been proposed to travel the retrograde transport route in association with membrane microdomains/lipid rafts (11). Indeed, it has been reported that Shiga toxin is associated with detergent resistant-membranes in compartments all along its retrograde pathway (12).

For the protein toxin to reach the ribosomes in the cytosol [for review see (13,14)], the endosome-to-Golgi transport step is crucial, as it determines the escape from lysosomal targeting and degradation. Many endogenous cargo molecules are retrieved from endosomal compartments to the *trans*-Golgi network, including the transmembrane proteins mannose-6-phosphate receptor (M6PR), TGN38 and furin, and the list of proteins being implicated in retrograde trafficking is increasing. Retrograde endosome-to-Golgi transport of Shiga toxin has been shown to depend on clathrin, dynamin and epsinR (9,15), be regulated by Rab6a′ (16), and to involve golgins (17,18) and the SNARE proteins Syntaxin 5 and 16 (19,20) for vesicle fusion at the *trans*-Golgi network. Recent

reports implicate retromer components, thus possibly the retromer complex in sorting of Shiga toxin in the retrograde direction (21–23). Importantly, also kinases such as p38α (24) and protein kinase C (PKC)δ (25) can regulate this transport step. However, it has become clear that there is more to retrograde sorting and transport of Shiga toxin than what can be explained by the action of regulatory proteins alone. Gb3 has, in addition to its requirement for Shiga toxin binding, been suggested to play a role in retrograde transport from endosomes to the Golgi apparatus, more specifically that a certain fatty acyl chain length of Gb3 favors sorting of internalized Shiga toxin in the retrograde direction (1,5,26,27). Studies of cells sensitized to Shiga toxin by butyric acid treatment, and comparison of cells with different toxin sensitivities, indicate that Gb3 with certain fatty acids, such as 16:0 is important for endosome-to-Golgi transport (1,5,26,27). However, under the conditions used and in the cell types previously studied, it is likely that also the protein composition is different (cell types of different origin) and that composition of other membrane lipids might be affected by butyric acid treatment. Furthermore, one might consider whether the fatty acid tail of other glycosphingolipids related to Gb3 and possibly present in the same membrane domain could play a role. We therefore set out to investigate whether inhibition of glycosphingolipid synthesis with PDMP (DL-threo-1-phenyl-2-decanoylamino-3-morpholino-1-propanol) or FB1 (Fumonisin B_1) in a more specific way could provide information about the role of lipids in endosome-to-Golgi transport. We have here studied the retrograde transport of Shiga toxin in HEp-2 cells under conditions where glycosphingolipid synthesis is inhibited for a relatively short time, in order not to induce a strong reduction of Shiga toxin binding to cells.

The experiments demonstrated that upon inhibition of glycosphingolipid synthesis with PDMP and FB1, glycosphingolipid species disappear from the cell with different rates. PDMP-treatment affected the composition and content of glycosphingolipid only, while other lipid profiles were not perturbed. In contrast, FB1 altered the profiles not only of ceramide, sphingomyelin and glycosphingolipids, but also glycerophospholipids, including plasmalogens. The data presented show the composition of a large part of the lipidome of HEp-2 cells both under normal growth conditions and under conditions where endosome-to-Golgi transport of Shiga toxin is 10-fold inhibited.

Results

Treatment of HEp-2 cells with PDMP and FB1 inhibits endosome-to-Golgi transport of Shiga toxin

HEp-2 cells were in these experiments treated with the drugs for different periods of time, and a number of parameters such as toxin binding, endocytosis, Golgi transport and toxicity were investigated. After 24 h with PDMP (1 μM) or after 48 h in the presence of FB1 (10 μM) there was, as described below, little effect on toxin binding and endocytosis, but a large effect on intracellular transport of Shiga toxin to the Golgi apparatus as well as a strong protection against the toxin. By quantifying Shiga B sulfation (a process occurring in the Golgi), after treatment of the cells with 1 μM PDMP for 24 h or with 10 μM FB1 for 48 h, we found that there was a strong reduction (about 10-fold) in the transport of Shiga B to the Golgi apparatus (Figure 1A). This effect was specific for Shiga B, no reduction was found when transport of ricin with a sulfation site was investigated under similar conditions (Figure 1B). Importantly, the less efficient transport of Shiga toxin to the Golgi apparatus was not a consequence of reduced toxin uptake. As shown in Figure 2A the endocytic uptake of the toxin after 45 min uptake was only reduced to about half. After 2 h incubation with toxin there was an even smaller difference, PDMP only reduced the amount of toxin taken up with about 30% (not shown). Also, when binding of the toxin was measured at low temperature to prevent internalization, the treatment with inhibitors maximally gave a 30–40% reduction under the conditions used (Figure 2B), and part of the apparent inhibition was due to a slight inhibition of cell growth caused by the incubation with FB1 (about 20–30%). In agreement with a recently published investigation (28) of the effect of glycosphingolipid synthesis inhibition in HeLa cells, we found that the treatment with PDMP reduced somewhat the association of surface-bound Shiga toxin with detergent-resistant membrane domains and with a similar reduction of endocytosis. In contrast to Shiga uptake, the transferrin endocytosis occurred at a normal rate (not shown) revealing that this pathway was unperturbed. In conclusion, our data indicate that both PDMP- and FB1-treatment efficiently reduce the transport of Gb3-bound toxin from endosomes to the Golgi apparatus (4–6 times reduction). This conclusion is supported by confocal microscopy studies of toxin uptake, which clearly reveal that there is less colocalization of both Shiga toxin and Shiga toxin B subunit with the Golgi marker giantin after treatment with PDMP and FB1 (Figure 3). Since the A-moiety of Shiga toxin can affect its transport (10), both were checked.

As shown earlier in HeLa cells (25) and HEp-2 cells (29) a fraction of internalized Shiga toxin is colocalized with EEA1-positive endosomes. These endosomes are likely to be relevant for retrograde transport of Shiga toxin (29), and we therefore investigated the possible effect of PDMP-treatment on this colocalization. As shown in Figure 4, PDMP did not have any significant effect on this colocalization, but it should be noted that only a very small fraction of the toxin was found in these endosomes. We then asked the question: What happens to the toxin in cells where Golgi transport is inhibited by PDMP? Does a larger fraction of the toxin end up in lysosomes? In cells which are normally resistant to Shiga toxin, the toxin is mainly transported to lysosomes (12,30). However, treatment with PDMP did

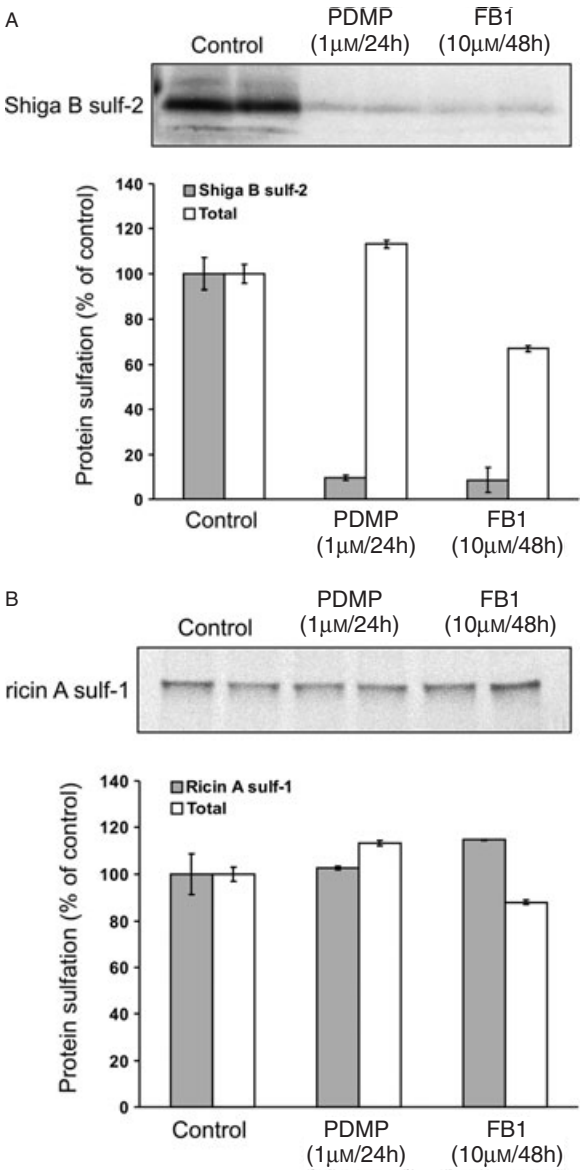

Figure 1: Retrograde transport of Shiga toxin, but not ricin, to the *trans*-Golgi network is blocked upon inhibition of sphingolipid synthesis. After incubation with inhibitors as indicated in the figure (1 μM PDMP for 24 h, 10 μM FB1 for 48 h), HEp-2 cells were preincubated with radioactive sulfate in MEM for 3 h at 37°C before incubation with Shiga B sulf-2 or ricin sulf-1 in the same medium for 45 or 120 min, respectively. Shiga B sulf-2 and ricin sulf-1 were immunoprecipitated from the cell lysates with anti-Shiga like toxin 1 or anti-Ricinus communis lectin antibody, respectively, immobilized on protein A-Sepharose beads. Immunoprecipitated protein was investigated by SDS-PAGE followed by autoradiography and degree of toxin sulfation, i.e. the amount of toxin having reached the *trans*-Golgi network, was determined by densitometric analysis of band intensities (gray bars). Total cellular protein sulfation was measured as 5% TCA-precipitated ^{35}S radioactivity (white bars). Results shown are representative of three independent experiments, and bars represent average deviations between parallels. Shiga B sulf-2 sulfation (A), but not ricin sulf-1 sulfation (B) is strongly reduced upon PDMP- or FB1-treatment.

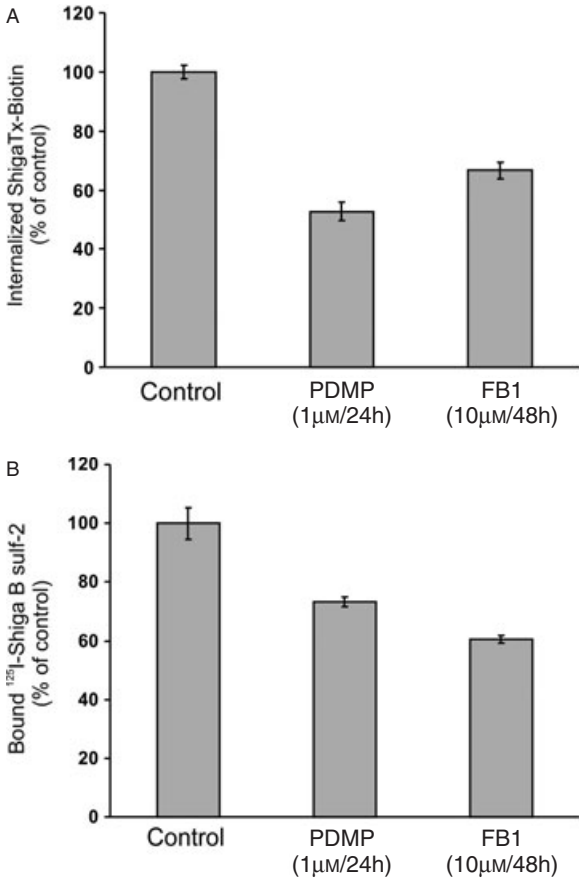

Figure 2: Uptake and binding of Shiga toxin after treatment with PDMP and FB1. After incubation with inhibitors as indicated on the figure (1 μM PDMP for 24 h, 10 μM FB1 for 48 h), binding and endocytosis were measured as described. (A): HEp-2 cells were incubated for 45 min with Shiga toxin-SS-Biotin before cell-surface bound Shiga toxin-SS-Biotin was treated with MESNa as previously described (25). After solubilization of the cells Shiga toxin-SS-Biotin was fished out from cell lysates and labeled by gentle shaking with 0.1 mg/mL streptavidin-coated magnetic beads and 0.5 μg/mL BV-TAG-labeled anti-Shiga like toxin 1 antibody in assay diluent (0.2% BSA, 0.5% Tween-20 in PBS) for 1.5 h. 'Control' in the figure stands for HEp-2 cells not exposed to inhibitors, but treated with MESNa (B): HEp-2 cells were incubated for 20 min on ice with ^{125}I-Shiga B sulf-2 (5×10^6 cpm/mL). Cells were washed, extracted with 5% TCA, and the precipitate dissolved in 0.1 M KOH. Radioactivity was measured on a γ-counter. Means (± SEM) of four independent experiments are shown. Shiga toxin binding impaired in both PDMP- and FB1-treated cells, but not enough to explain the observed protection.

not increase, it rather significantly ($p < 0.01$) decreased the fraction of toxin found in organelles that are positive for the lysosomal marker LAMP1 (Figure 4). Similar results were obtained with FB1 treatment (data not shown). Our data are in agreement with earlier studies where Shiga toxin transport to the Golgi is inhibited by knockdown of proteins important for retrograde transport; the toxin seems to end up in EEA1- and LAMP1-negative

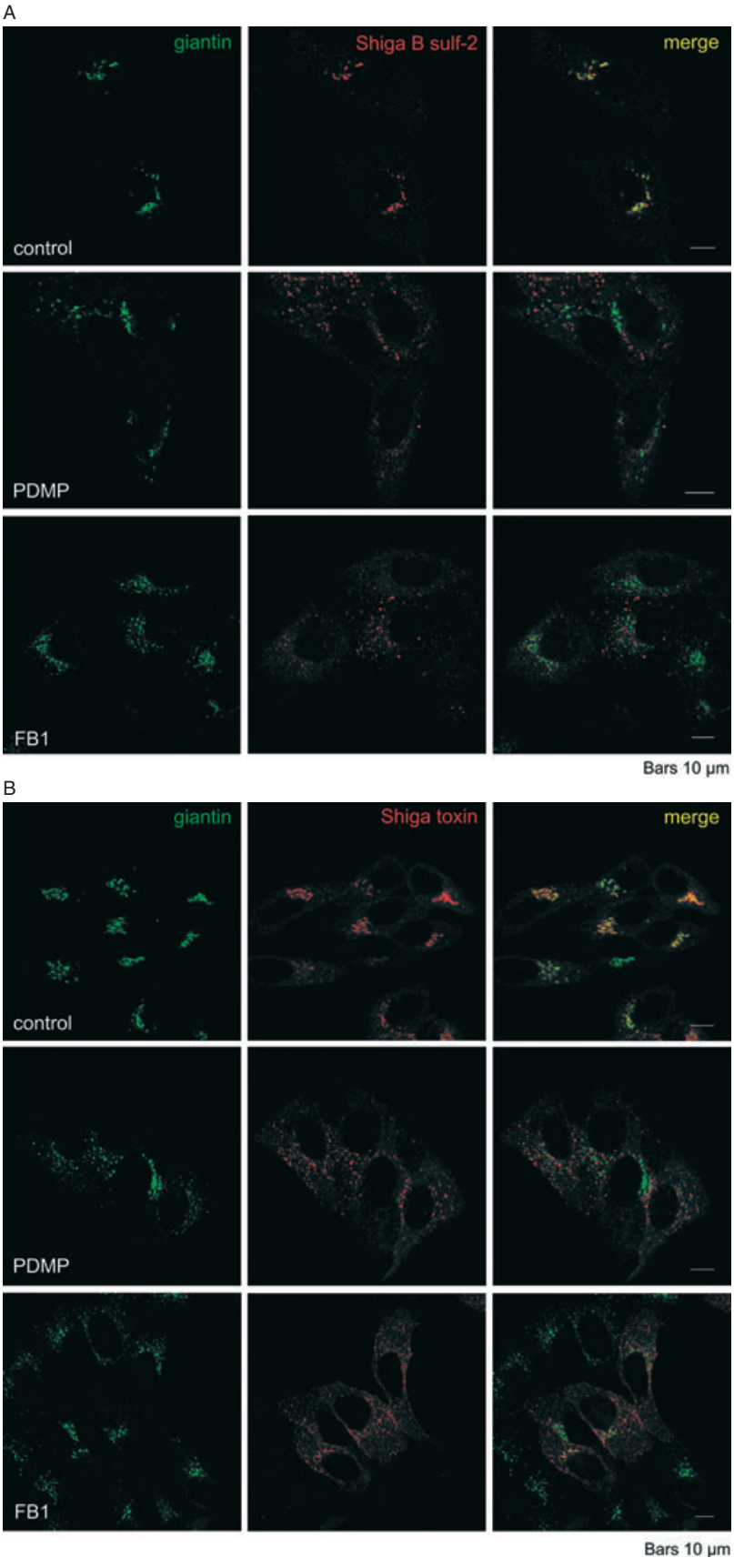

Figure 3: Shiga toxin can not be visualized in the Golgi apparatus upon inhibition of glycosphingolipid synthesis. Shiga toxin (A) or Shiga B sulf2 (B) was internalized constitutively for 45 min at 37°C into HEp-2 cells which had been preincubated with 1 µM PDMP for 24 h or 10 µM FB1 for 48 h. After fixation and permeabilization (0.2% Triton X-100), cells were stained for Shiga toxin and the Golgi marker giantin, mounted in Mowiol and investigated by confocal microscopy. Under control conditions, Shiga toxin colocalizes extensively with giantin, whereas upon both PDMP- and FB1-treatment, no colocalization is observed.

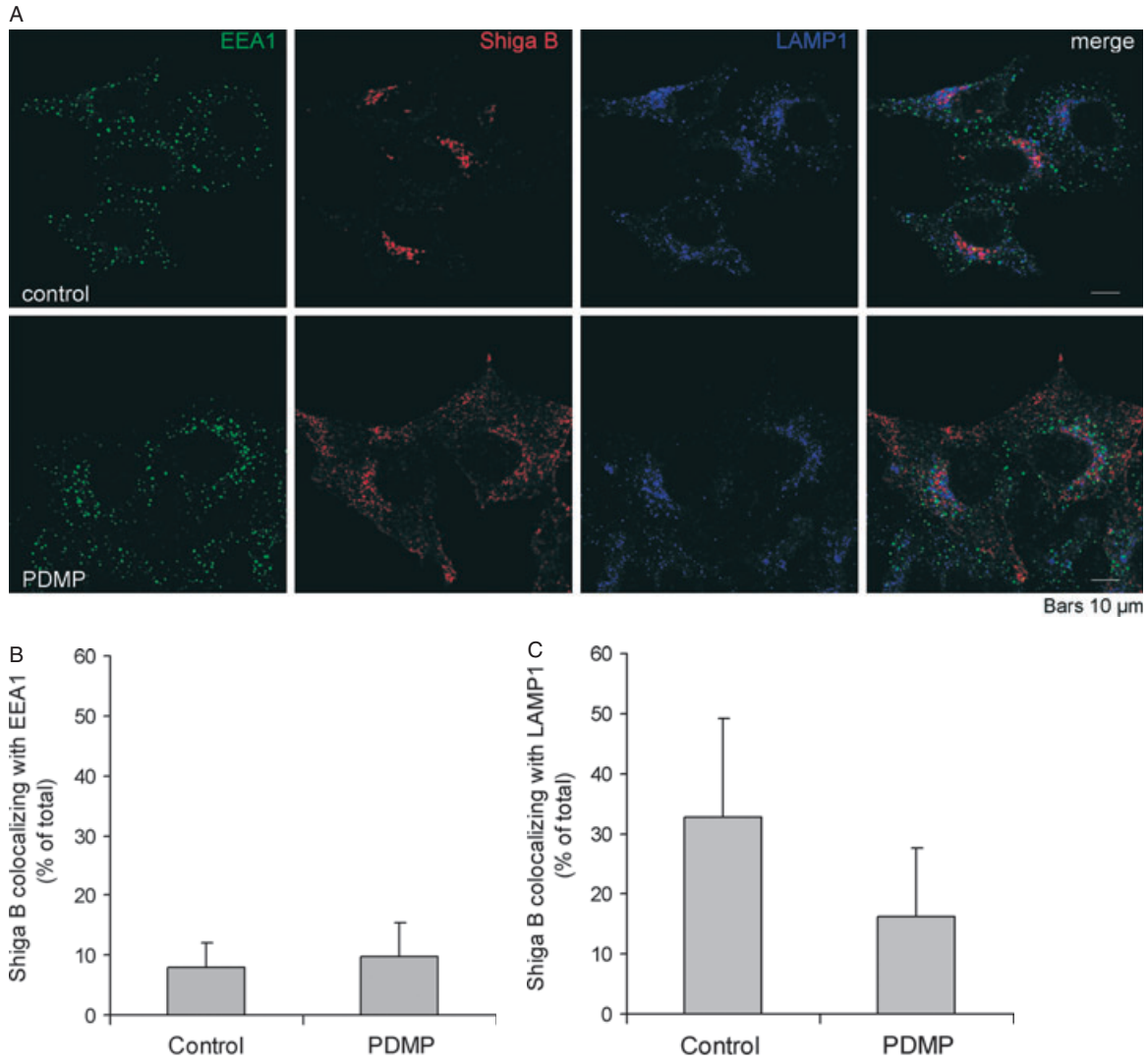

Figure 4: Treatment with PDMP does not increase the degree of colocalization between Shiga toxin B subunit and EEA1- or LAMP1-positive structures. HEp-2 cells were incubated with or without PDMP (1 μM, 24 h), before incubation with Alexa Fluor 555-labeled Shiga B for 45 min at 37°C. After fixation and permeabilization, cells were co-stained with antibodies against early endosome marker EEA1 and lysosomal marker LAMP1 (A). Quantification of colocalization was performed using LSM Image Browser software, and shows that the degree of colocalization between the Shiga B subunit with EEA1 (B) remains unchanged, while there is a significant decrease ($p < 0.01$) in the colocalization with LAMP1 (C), when comparing cells treated with PDMP with untreated cells. $n = 21$ for control and $n = 18$ for PDMP.

endosomes or transport vesicles unable to fuse with the Golgi apparatus (25,31,32). Our results raise the question of whether PDMP-treatment affects the localization of sorting nexins involved in retrograde transport of Shiga toxin (21–23). Interestingly, as shown in Figure 5, PDMP-treatment significantly ($P < 0.01$) changed the cellular localization of Sorting nexins 1 and 2 (SNX1 and SNX2) in a similar manner as reported for SNX1 after EHD3 knockdown (32). Treatment with the inhibitor PDMP induced a relocalization of the two sorting nexins from the Golgi area to endosomal localization. This change is likely to be associated with the observed reduction in retrograde transport.

Treatment of cells with PDMP and FB1 protects cells against Shiga toxin

When HEp-2 cells were incubated with PDMP and FB1 there was with time an increasing protection against intoxication with Shiga toxin. A short incubation (4 h) with the inhibitors provided essentially no protection (1.5 times protection with PDMP, no protection with FB1), whereas increasing protection was obtained after longer incubation times. Representative curves for inhibition with 1 μM PDMP for 24 h and with 10 μM FB1 for 48 h are shown in Figure 6. Apparently, the protection against the toxin was even stronger than the inhibition of Golgi transport, suggesting additional effects on later transport steps, in

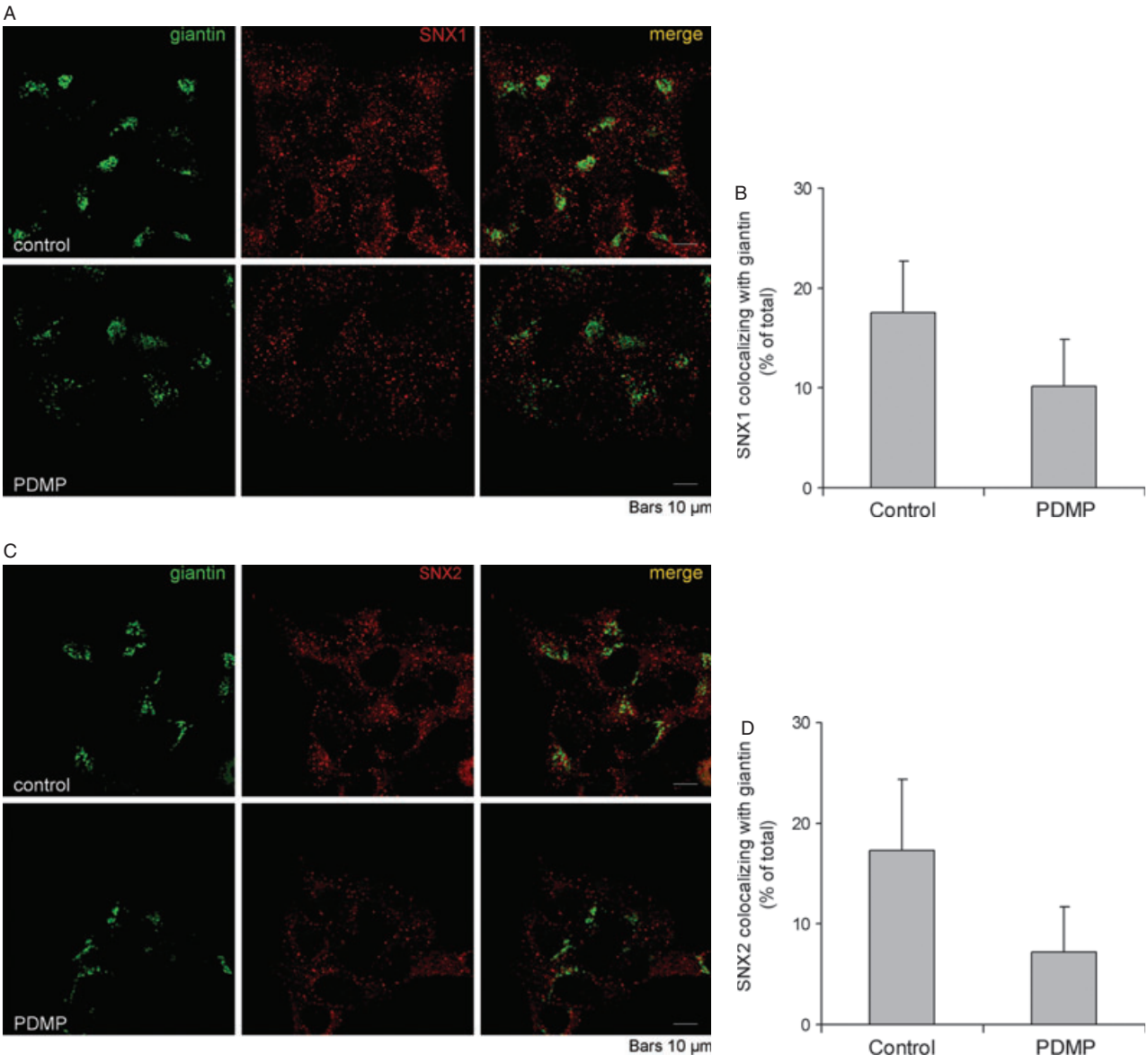

Figure 5: SNX1 and SNX2 show less colocalization with the Golgi apparatus upon treatment with PDMP. After incubation of HEp-2 cells with PDMP (1 µM, 24 h), cells were fixed, permeabilized and co-stained for the Golgi marker giantin and either of the retromer components SNX1 (A) or SNX2 (C). Quantitative analyses performed using LSM Image Browser software reveal that cells treated with PDMP display significantly less colocalization ($p < 0.01$) between SNX1/SNX2 (B, D) and Golgi than control cells. For SNX1, $n = 21$ for control and $n = 23$ for PDMP. For SNX2, $n = 24$ for both control and PDMP.

agreement with a report on HeLa cells where lack of glucosylceramide apparently affected ER translocation to the cytosol [(28), and see discussion]. Again, as shown earlier where Golgi transport was quantified by measuring sulfation, PDMP and FB1 did not affect the toxicity of the related toxin ricin (not shown). In theory, a protection against Shiga toxin could also be caused by a reduced nicking of the A-moiety of the toxin, a process ascribed to the cellular enzyme furin which cleaves and activates Shiga toxin, optimally at low pH (33). However, by using ^{125}I-labeled Shiga toxin we found that treatment of HEp-2 cells with PDMP had no effect on toxin processing (not shown), and the protection by PDMP was also observed when we precleaved the toxin with trypsin before addition to cells (data not shown).

The lipidome of HEp-2 cells treated with PDMP and FB1

The impact of glycosphingolipid depletion in HEp-2 cells on the intracellular transport of Shiga toxin was investigated by interrupting the glycosphingolipid biosynthesis by the two inhibitors PDMP and FB1. To analyze the corresponding changes in cellular lipids, cells were incubated for 4, 24 and 48 h with 1 µM

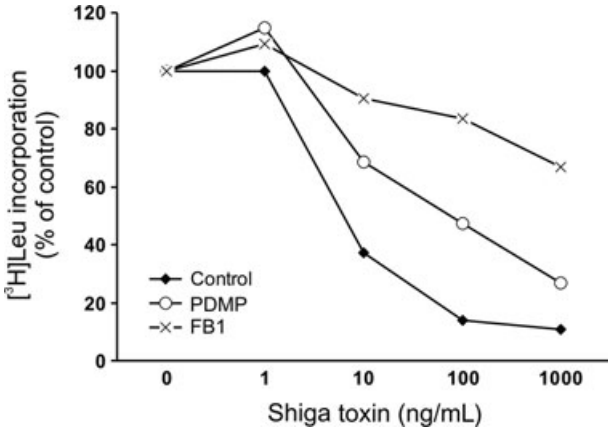

Figure 6: Inhibition of glycosphingolipid synthesis protects cells against Shiga toxin cytotoxicity. HEp-2 cells were incubated with or without the PDMP (1 μM for 24 h) or FB1 (10 μM for 48 h). They were then incubated for Shiga toxin for 2 h, and at the end of this incubation the medium was removed and the incubation was continued in leucine-free Hepes-buffered medium containing [^{3}H]leucine for 20 min at 37°C. The cells were extracted with 5% TCA, and the precipitate was dissolved in 0.1 M KOH. Radioactivity was measured on a β-counter. The result is representative of three independent experiments; error bars not included, average deviations are < 10%. On average, PDMP-treatment gives 6.5 times protection (based on the concentrations required to give 50% inhibition of protein synthesis), whereas treatment with FB1 gives more than 230 times protection.

PDMP or 10 μM FB1 and then their total lipid extracts were analyzed by mass spectrometry (MS) (34). This approach was used to identify and quantify 135 species from the major lipid classes phosphatidylcholines (PCs), phosphatidylethanolamines (PEs) and sphingomyelins (SMs), and principal component analysis of these data (Figure 7A) revealed that major changes in the lipidome for FB1-treated cells compared to the control cells was established after 24 h of incubation due to decrease in concentrations of SMs and PC-Os species and increase in abundance of PE species (Figure 7B; only 75 of the major species are shown as detailed in the figure legend). At the same time, the lipidome profile of PDMP-treated cells was not altered substantially (Figure 7A,B). As expected, interfering with the ceramide biosynthesis with FB1 and the HexCer biosynthesis with PDMP, resulted in a time-dependent decrease of glycosphingolipids; the data obtained at all three time-points for control cells and as well as cells incubated with each of the inhibitors are shown for Cer, HexCer, and Gb3 in Figure 8 and for SM and LacCer in Figure S1. The apparent decrease in lipid content differed for the two inhibitors not only with respect to the total lipid content of each class, but interestingly the changes were species-dependent, being affected by their *N*-amidated fatty acid moieties (Figure 8 and Figure S1). For all monitored sphingolipids the 24:1 fatty acid species were the most abundant. Gb3s with 24:1 fatty acid moiety constituted 50 mol% of total Gb3, whereas species with 16:0, 22:0, 22:1 and 24:2 fatty acids constituted 16%, 8%, 12% and 11%, respectively (Table 1 and Table S1).

In cells incubated with PDMP, HexCer species were most rapidly depleted (Figure 8). After 24 h incubation with PDMP, approximately 2-fold reductions of total HexCer, LacCer and Gb3 content were observed compared to the control cells (Figure 8 and Table S2). The depletion was relatively independent of the fatty acid moieties, although species with the fatty acid 16:0 were degraded faster and to a larger extent than 24:1. Altogether, the lipid profiles of cells incubated with PDMP for 24 or 48 h were very similar. As expected, PDMP did not cause any significant changes in the levels of Cer or SM (Figure 8 and Figure S1).

The FB1-induced sphingolipid and ceramide depletion was also dependent on the *N*-amide fatty acid moiety. Species containing the fatty acid 16:0 were depleted preferentially (Figure 8 and Figure S1). For HexCer and Gb3, treatment with FB1 for 24 h reduced the content of the species with fatty acid 16:0 to similar levels as PDMP, while for 24:1 species of HexCer, LacCer and Gb3 it took 48 h to reach similar levels as PDMP (Figure 8 and Figure S1). FB1, in contrast to PDMP, caused a variety of changes in the lipidome.

As shown in Figure 8, there was a slight decrease per cell of ceramide, hexylceramide and Gb3 even in control cells with time. This is most likely due to a change in cell density during the 48 h of incubation with and without inhibitors. Increasing cell density might change the cell shape as well as affect the level of lipids. It should, however, be noted that all the cells were equal at time zero (seeded at the same time and transferred to the medium with and without inhibitors at time zero). Importantly, control values were measured at each time point.

Discussion

In the current article we show that transport of Gb3-bound Shiga toxin to the Golgi apparatus is reduced in HEp-2 cells upon inhibition of glycosphingolipid synthesis. Interestingly, the toxin does not get stuck in EEA1-positive endosomes or in LAMP1-positive lysosomes, but rather in vesicular structures that could be transport vesicles. Furthermore, we show that upon inhibition of glycosphingolipid synthesis with PDMP and FB1 the fraction of the different lipid species left in the cell, such as HexCer, Gb3 and SM, not only varies with time as expected, but also species disappear at different rates, most likely by degradation in lysosomes (35). Previous studies of Shiga toxin intoxication have indicated the importance of the *N*-amide fatty acid moiety in Gb3 (1,5,6,27,36). The first demonstration of retrograde transport to the ER of Shiga toxin was performed by sensitizing A431 cells to the toxin by butyric acid treatment (1), and it was found that the sensitizing effect

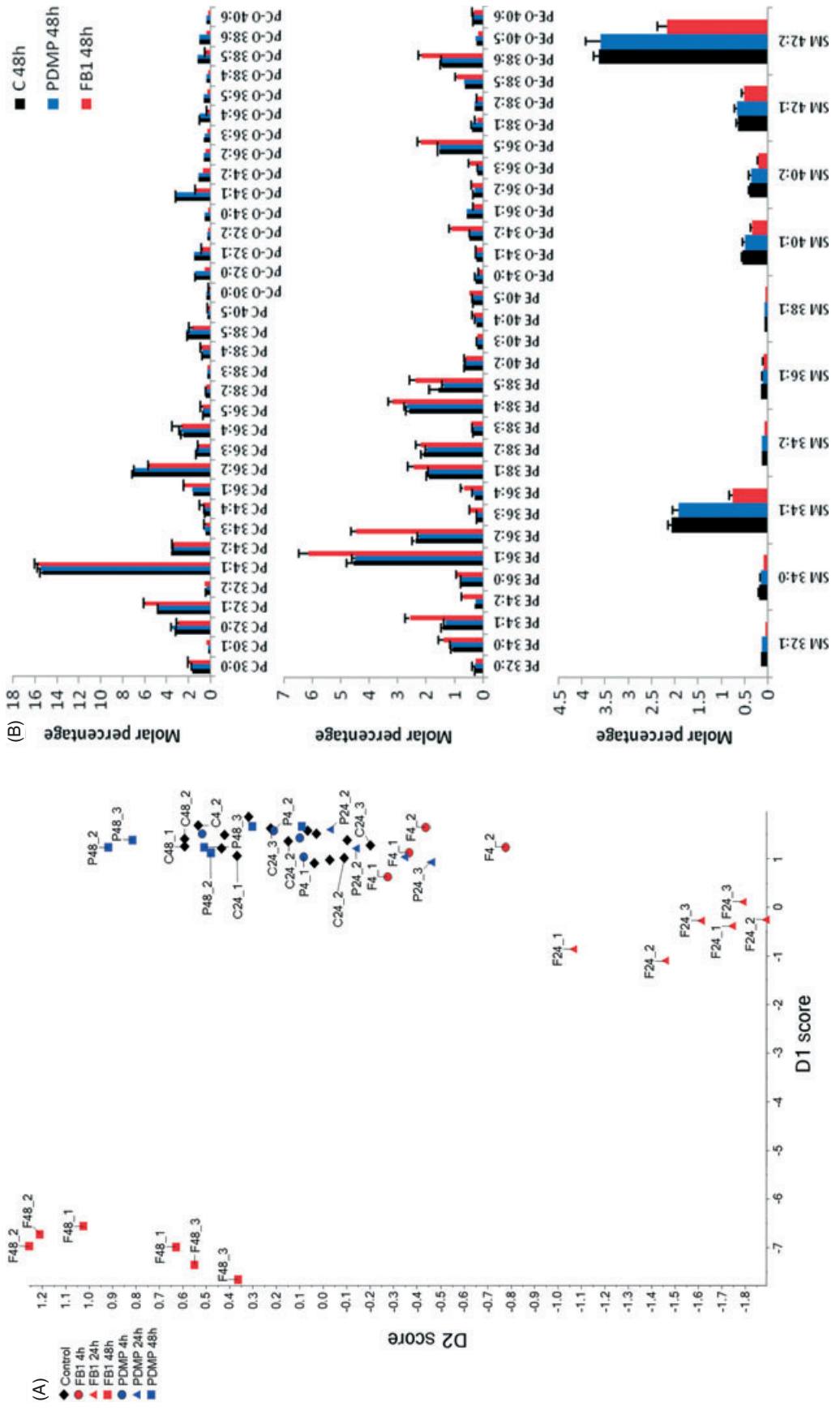

Figure 7: Response of the HEp-2 lipidome after inhibition of glycosphingolipid synthesis by PDMP and FB1. (A) Principal component analysis of 135 major membrane lipids after treatment with PDMP (1 μM for 24 h) or FB1 (10 μM for 48 h). All data with control cells are black, data obtained after incubation with PDMP are blue, and data obtained after incubation with FB1 are red; circles show 4 h data, triangles show 24 h data and squares show 48 h data. The last number indicates the number of the three replicate samples, and each sample was analyzed twice to monitor the MS variability in the principal confocal analysis. (B) Comparison of lipid profiles after treatment with 1 μM PDMP or 10 μM FB1 for 48 h. The species shown are only those above 0.2 mol% for PE and PC and above 0.1 mol% for SM.

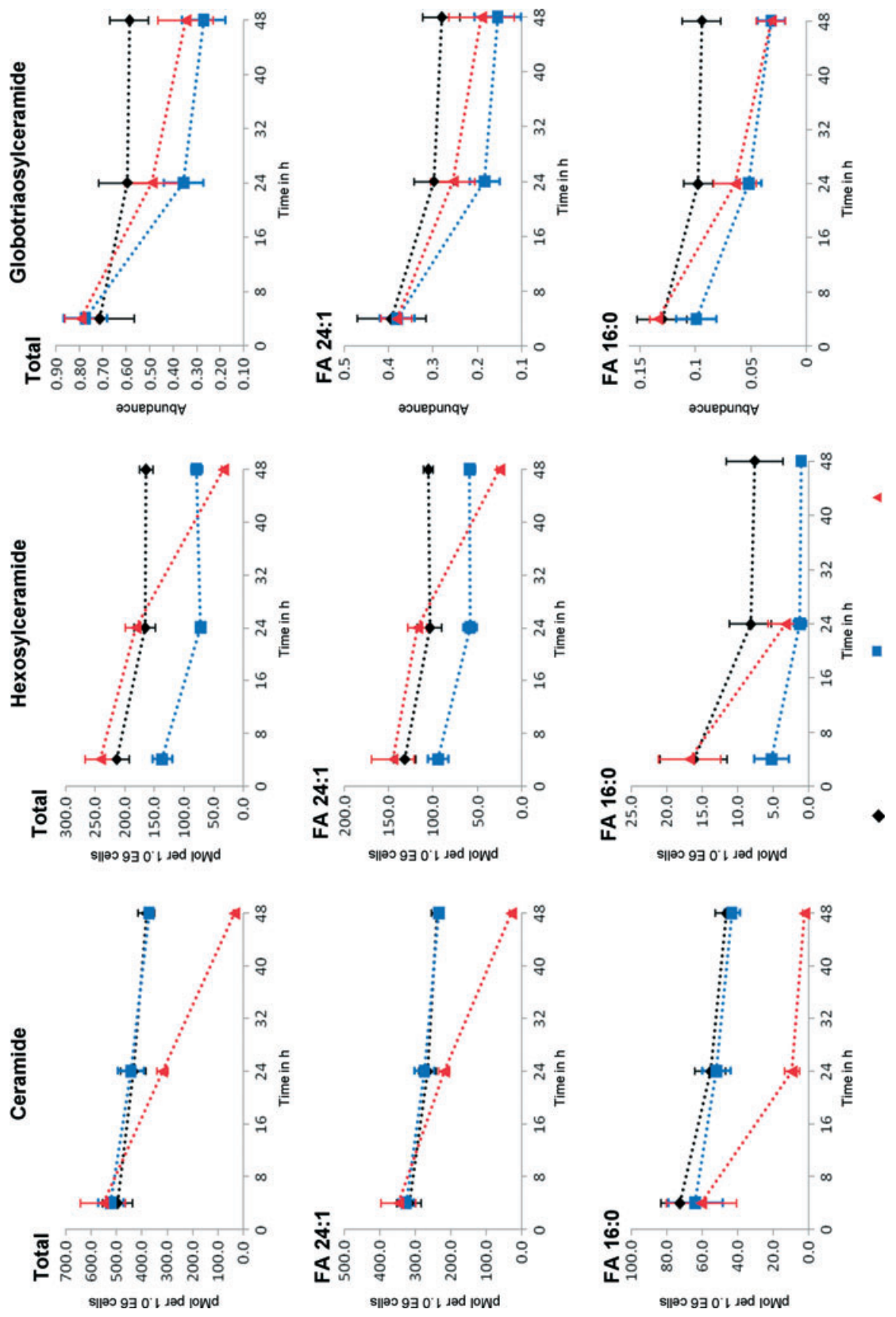

Figure 8: Depletion of sphingolipids of HEp-2 cells upon incubation with PDMP and FB1. Absolute quantification of Cer (left column), HexCer (middle column) and TriHexCer (Gb3; right column) in HEp-2 cells are shown after treatment with 1 μM PDMP for 24 h (blue squares), 10 μM FB1 for 48 h (red triangle) and for control cells (black rhombus). Absolute quantities for total class (top row), species with N-linked fatty acid 24:1 (middle row) and species with N-linked fatty acid 16:0 (bottom row) are displayed.

Table 1: Percent of different fatty acid chain length of Gb3 species in different cell types

Chain length of fatty acid	HEp−2[a]	HeLa[b]	XF−498[c] Astrocytoma	SKOV3[c] Ovarian cancer
24:1	50	8	7	15
Other 24	11	42	32	12
22	20	35	11	8
20	<3	–	1	2
18	<3	4	23	28
16	16	6	20	28

[a]Present study.
[b]Ref. (28).
[c]Ref. (26).

was dependent on new glycosphingolipid synthesis (27), giving rise to Gb3s with different fatty acids. Furthermore, a comparison of Gb3 in cells with different sensitivity seemed to underscore the importance of the 'right' type of Gb3 for Golgi transport to occur (1,36). However, in the previous studies also the fatty acids in other lipid species might vary, but were not measured.

The bulk of Gb3, HexCer and LacCer contain long chain fatty acid moieties, with 24:1 being the most abundant species. Upon inhibitor treatment most of the depletion of sphingolipid molecules was due to depletion of these long chain fatty acid species. However, it should be noted that the 16:0 species in general were depleted faster than the 24:1 species. There is a more rapid and extensive depletion of HexCer with the fatty acid 16:0 than HexCer with 24:1 when glycosphingolipid synthesis is blocked with PDMP, and the effect of PDMP on Gb3 was also observed earlier with 16:0 (after 4 h) than with 24:1 (after 24 h). It should be noted that only a small fraction of the cell-associated toxin is transported to the Golgi; it is therefore possible that minor lipid species can bring the toxin to the Golgi.

It is conceivable that HexCer with 16:0 might play an important role for sorting in the direction of the Golgi apparatus. In fact, among the lipid species analyzed in the present study, the HexCer species with the fatty acid 16:0 was the single species that decreased by a similar factor as the change in toxin transport to the Golgi apparatus (measured as sulfation of the Shiga B subunit). To our knowledge, it is not known how much Gb3 versus HexCer that is present in early/sorting endosomes or in the recycling compartment from where Shiga is sent to the Golgi apparatus. However, since HexCer is synthesized in the Golgi it would not be surprising to find a certain fraction of this glycosphingolipid also in a compartment communicating directly with the Golgi apparatus. It should also be kept in mind that the relative composition of Gb3 and HexCer species most probably are not uniformly distributed in the different cell membranes and that there may be a critical local concentration that is of importance for the intracellular transport of Shiga toxin.

The possibility existed that a change in glycosphingolipid-composition or glycosphingolipid levels would change the cellular amount of cholesterol which in itself has been shown to be important for Golgi transport of Shiga toxin. However, this was not the case [our unpublished data, which are in agreement with studies on NIH 3T3 cells (37)]. This conclusion is also in agreement with the finding that cholesterol is important for ricin transport to the Golgi (38), but no effect of PDMP or FB1 treatment was observed on sorting of ricin to the Golgi apparatus. Thus, not all types of Golgi transport are affected. We have previously shown that ricin transport to the Golgi does not have the same requirements as Golgi transport of Shiga toxin, for instance, there is not any requirement for endosomal clathrin (9). There are different pathways between early endosomes and the Golgi apparatus, which was recently supported by the report from Zhao Lieu et al. (39). They published that Shiga toxin B fragment is transported to the Golgi by a different mechanism than TGN38 and mannose-6-phosphate receptors, which in contrast to Shiga B required the protein GCC88 for Golgi transport.

It is known that the fatty acids in glycosphingolipids affect rigidity of the membrane and thereby its ability to form tubules and buds as well as to fuse. Furthermore, detergent-resistant membrane domains with lipids containing C16 and C18 fatty acids are believed to be thicker than domains with longer fatty acids (40). Such a difference might be important for the shape of an organelle and membrane sorting. It is known that clathrin (9,15), as well as sorting nexins 1 and 2 are important for Golgi transport of Shiga (21–23). The possibility exists that sorting nexins might be differentially recruited to internal membranes after changes in the lipid composition and alterations in the curvature of parts of the endosomes (the BAR domain in sorting nexins binds to membranes in a curvature-dependent manner) (41). However, we cannot exclude the possibility that the changes observed in localization of SNX1 and SNX2 upon PDMP-treatment might reflect a change in sorting caused by another component of the transport machinery. Furthermore, the fact that the clathrin-dependent uptake of transferrin at the cell surface functions normally is not a guarantee for normal clathrin-dependent functions at intracellular organelles. If there is a dynamic regulation of protein complexes associated with endosomes, one may not be able to discover all types of differences by studying isolated endosomes. Dissociation of proteins as well as changes of morphology may occur during the fractionation procedure. Therefore, although we did not observe any significant changes after incubation with PDMP by western blotting of the retromer component Vps26 and arrestin (29) on isolated endosomes (our unpublished results), this could be due to the fact that Vps-proteins can be found on long tubular extensions that detach before transport to the Golgi and that might be lost or changed during isolation.

Shiga toxin transport between endosomes and the Golgi is not only regulated by coat proteins and sorting nexins, but toxin-induced signaling also turns out to be important. We have recently found that both the Shiga-induced activation of PKCδ (25) and the activity of mitogen-activated protein (MAP) kinase p38α (24) are important for Golgi transport. Whether Shiga signaling is dependent on the type of Gb3/HexCer present has not yet been investigated, but would not be surprising since the occupancy of Shiga-Gb3 complexes in lipid rafts and the right type of lipids present could be a prerequisite for the toxin-induced signaling and ability to mediate its own transport. Future studies are needed to fully understand why the changes in glycosphingolipids here observed have such a large effect on Shiga toxin transport.

The present data show, as mentioned earlier, a more rapid decline in the cellular level of HexCer and other lipids containing the *N*-amidated fatty acid 16:0 than for those with 24:1. That such differences can occur is not surprising as it has been reported that the lipid tail can affect sorting of a certain lipid in cells. Thus, Mukherjee et al. (42) reported that $DiIC_{16}(3)$, a synthetic lipid analog containing two 16 carbon atom chains without any double bonds, following endocytosis entered into late endosomes, whereas the similar analog with 18 carbon atoms and two double bonds was mainly found in the recycling compartment and thus to a smaller extent was sent to degradation. Their data thus fit with our results, showing a more rapid disappearance of 16:0 species of Cer, SM and some glycosphingolipids than of the corresponding species containing the longer unsaturated fatty acid 24:1. Koivusalo et al. (43) reported a larger extent of recycling to the plasma membrane of the SM species containing 15:0 than of the one with 21:0. It is difficult to compare their finding with the present data as they studied only species with saturated fatty acids or synthetic pyrene analogs. It should also be noted that we did not see any effects on SM following incubation with PDMP and that surprisingly small effects were observed for some SM species (such as 24:1; Table 1) even after incubation with FB1 for up to 48 h. Interestingly, it was also reported (44) that transport of BODIPY-LacCer upon inhibition of glycosphingolipid synthesis was rerouted from endosomes-to-Golgi transport and instead ended up in lysosomes.

The finding that FB1 gives essentially the same changes in transport of Shiga as treatment of cells with PDMP is comforting in the sense that no specific intermediate accumulation after treatment with one or the other is important for the conclusions drawn. However, the fact that FB1 treatment changes a large number of different membrane lipids is interesting in itself seen from the viewpoint of lipid synthesis and degradation, and the influence one might have on other lipid components of the membrane by adding FB1. The stronger protection against Shiga toxin provided by FB1 compared with PDMP could be due to its ability to inhibit synthesis of ceramide or sphingomyelin species which might be important for lipid organization along the retrograde pathway. However, since so many other changes in lipid composition occur in the presence of FB1, different changes might contribute to the less efficient transport of Shiga toxin into the cytosol. The consequences of adding FB1 is of course also of interest in connection with its ability to contaminate food and induce cancer in humans (45).

Although the changes observed in lipid composition following incubation with FB1 is somewhat outside the main scope of this article, it warrants some comments. The data in Figure 7B show that a large number of the PE and PE-O species show an increase (average of approximately 30%) following incubation with FB1 for 48 h. The content of a few species, all with rather short chains, almost doubled (e.g. PE 34:2, PE 36:2 and PE-O 34:2), whereas PE or PE-O species with 40 carbons or more remained unaffected. For PC-O considerable decreases (25–65%) were observed for most species after incubation with FB1 for 48 h, independently of fatty acid moieties. For the PC species there were only minor changes for a few species (e.g. 20–25% decrease in PC 36:2 and as similar increase in PC 32:1). To our knowledge, this is the first report on how a large part of the lipidome is affected by FB1 treatment. Smith and Merrill (46) reported a 30% increase in total PE and an increase of 10% in total PC following incubation of J774A cells with 50 μM FB1 for 12 h. Their data for total PE is thus in agreement with our data, whereas we did not see any changes in total PC and found a major decrease in PC-O. We have no explanation as to why incubation with FB1 affects such a large part of the lipidome; but this effect obviously has to be taken into consideration when interpreting data from studies with this inhibitor.

The literature reveals that there are large cell type-dependent differences when it comes to the species of Gb3 present and involved in Shiga binding. As shown in Table 1 HEp-2 cells contain much more of 24:1 than the three other cell types listed, whereas the other cells contain much more of either other fatty acids with 24 carbon atoms (HeLa and XF-498), or 22 carbon atoms (HeLa), or 18 carbon atoms (XF-498 and SKOV3). It is therefore not surprising that the effects of blocking glycosphingolipid synthesis may vary.

Inhibition of glycosphingolipid synthesis in HeLa cells, for as short as 2 h, was reported to provide a strong protection against Shiga toxin, but apparently without any significant effect on retrograde transport of a Shiga B-KDEL construct (28). This rapid protection suggests that the mechanism behind the protection is different in HeLa cells from what we observe in the HEp-2 cells where it takes much longer time to obtain a protective effect. The lack of rapid protection is in agreement with recent studies of Lingwood et al. (47) showing that cell types differ, and that there is essentially no protection in several cell lines (including HEp-2 and HeLa) after short-term inhibition

of glucosylceramide synthesis. It should, however, be noticed that HeLa cells vary, there seems to be different strains. Also, these authors (47) could not confirm the glucosylceramide-requirement for Shiga toxin-localization to rafts reported by Smith et al. (28). Furthermore, studies of Shiga B with and without KDEL can be expected to give different results. Even though native Shiga B-chain and Shiga B-KDEL were reported to be transported with similar kinetics to the ER under normal conditions (48), this might not hold true when conditions are changed, for instance after blocking glycosphingolipid synthesis. Also, the KDEL construct can be expected to use COPI-coated vesicles for retrograde transport, whereas this is not the case for the native toxin (49,50), and a recent study of Shiga B with and without KDEL has revealed important differences (51). Importantly, it was demonstrated that crosslinking of the KDEL-receptors by Shiga B-KDEL leads to activation of Src family kinases (SFKs), a signaling that starts in the Golgi and spreads throughout the cell. The study showed that native Shiga B moved more slowly and that it did not affect the SFK-phosphorylation cascade induced by the KDEL construct. Clearly, different results have to be expected depending on the molecule studied. Furthermore, as described earlier, cell-type dependent differences are likely. Although at the time these differences seem to complicate the picture, these features might help in clarifying the principles behind membrane sorting, for instance along the retrograde pathway.

Our present data show that changes in glycosphingolipids can have large consequences for retrograde sorting, and the present study reveals the potency of advanced MS analysis of lipids when it comes to understanding transport at the molecular level. One may to a larger extent, than what has been done so far, have to address what happens also to lipids when one changes the cellular level of proteins involved in trafficking and sorting.

Materials and Methods

Reagents

Rabbit polyclonal anti-*Ricinus communis* lectin antibody and antibody to LAMP1 were from Sigma Chemical (St. Louis, MO, USA). Mouse monoclonal anti-Shiga like toxin 1 antibody was from Toxin technology (Sarasota, FL, USA). Rabbit anti-giantin was from Berkeley Antibody Company (Richmond, CA, USA). Cy2-conjugated donkey anti-rabbit immunoglobulin G (IgG) and Cy3-conjugated donkey anti-mouse IgG antibodies were from Jackson ImmunoResearch Laboratories (West Grove, PA, USA). Anti-EEA1 was a gift from Harald Stenmark, The Norwegian Radium Hospital, Norway. Anti-SNX1 and anti-SNX2 were from BD Biosciences (Erembodegem, Belgium). To label Shiga toxin B-K3 we used Alexa Fluor® 555 Monoclonal Antibody Labeling Kit (Invitrogen). Pre-cast polyacrylamide gels were purchased from Pierce Biotechnology (Rockford, IL, USA). [^{3}H]leucine was purchased from GE Healthcare (Princeton, NJ, USA), $Na_2^{35}SO_4$ from Hartmann Analytics (Braunschweig, Germany) and ^{125}I was from PerkinElmer (Norwalk, CT, USA). IODO-GEN Iodination Reagent was from Pierce Biotechnology. EZ-Link Sulfo-NHS-SS-Biotin was purchased from Pierce Biotechnology. Shiga toxin was provided by Dr J. L Koslov (Academy of Sciences of Russia, Moscow, Russia) and Dr J.E. Brown (USAMRIID, Fort Detrick, MD, USA). Ricin, PDMP, α-lactose, mercaptoethanesulphonic acid (MESNa), n-octyl β-D-glucopyranoside, Hepes, bovine serum albumin (BSA), butyric acid, Trizma Base, Triton X-100 and Tween-20 were purchased from Sigma Chemical. FB1 was purchased from Biomol International, Exeter, England. Complete ethylenediaminetetraacetic acid (EDTA)-free Protease Inhibitor cocktail tablets were from Roche Diagnostics (Indianapolis, IN, USA), and protein A-Sepharose was from GE Healthcare. Emulsifier-Safe scintillation fluid was from PerkinElmer. Synthetic lipid standards were purchased from Avanti Polar Lipids, Inc. (Alabaster, AL, USA). Chloroform, methanol, isopropanol, ammonium acetate and ammonia carbonate were of Liquid Chromatography grade and purchased from Fluka (Buchs SG, Switzerland) and Sigma-Aldrich Chemie GmbH (Munich, Germany). All other chemicals were from Merck (Whitehouse Station, NJ, USA), unless otherwise stated.

Equipment

Nunc Cell culture plates were purchased from Nalge Nunc International (Rochester, NY, USA). Gel-electrophoresis chamber and wet electroblot apparatus (Mini-PROTEAN 3 Electrophoresis System with Mini Trans-Blot Module), and Precision Plus Protein molecular weight marker were from BioRad Laboratories. Immobilon-P 0.45 μm polyvinylidene difluoride (PVDF) membrane was from Millipore. M1R Analyzer was from BioVeris Corporation (Gaithersburg, MD, USA). QuantifyOne 1-D Analysis Software was from BioRad Laboratories (Hercules, CA, USA). ImageQuant Version 5.0 software was from GE Healthcare. Packard Tri-Carb Liquid Scintillation Analyzer 2100TR β-counter was from PerkinElmer, and LKB Wallac 1261 Multigamma γ-counter was from Pfizer (New York, NY, USA). Eppendorf 5415C Micro Centrifuge was from Eppendorf (Hamburg, Germany).

Cell cultures and inhibitors

HEp-2 cells were maintained in Dulbecco's Modified Eagle Medium (DMEM) (Invitrogen, Carlsbad, CA, USA) supplemented with 10% fetal calf serum (PAA Laboratories, Linz, Austria), 100 U/mL penicillin and 100 μg/mL streptomycin (Invitrogen) at 37°C in a 5% CO_2 atmosphere. Experiments were performed with HEp-2 cells seeded into cell culture plates of indicated size and incubated with 1 μM PDMP or 10 μM FB1 for up to 48 h, as indicated in the results section. PDMP blocks glucosylation of ceramide by inhibiting UDP-glucose:ceramide glucosyltransferase (glucosylceramide synthetase), thus reduces cellular synthesis of complex glycosphingolipids. FB1, a mycotoxin produced by Fusarium moniliforme, is an inhibitor of ceramide synthase (sphingosine/sphinganine *N*-acyltransferase), thus blocking cellular formation of both ceramides, SMs and complex glycosphingolipids.

DNA constructs and molecular cloning

The vector encoding Shiga B sulf2, a recombinant modified version of the toxin, containing a tandem of sulfation sites, was a kind gift from Dr Bruno Goud, Institute Curie, Paris, France. Cloning of Shiga B-KKK: The Shiga B coding sequence was amplified using Pfx-DNA polymerase (Invitrogen, Carlsbad, CA, USA) with the following primers: 3′-CAT GCC ATG GCA AAA AAA ACA TTA TTA ATA GCT GC and 5′-CCG CTC GAG TTA TCA CTT CTT CTT ACG AAA AAT AAC TTC GC−3′. The resulting amplicon was then cut with *Nco*I and *Xho*I (underlined in the primer sequences) and cloned into pET21d (Novagen, Madison, WI, USA). The resulting plasmid was then sequence verified (Eurofins MWG Operon, Ebersberg, Germany) and transformed into BL21 codon + bacteria (Stratagene, La Jolla, California) for further protein expression. The proteins were produced and purified as previously described (9). Ricin A sulf 1 (a modified ricin A-chain containing one tyrosine sulfation site) was produced and reconstituted with the B-chain as described earlier (52).

Shiga toxin binding

Labeling of Shiga B sulf-2 with ^{125}I was performed by the iodogen method with the IODO-GEN Iodination Reagent (Pierce Biotechnology) according to protocol provided by the manufacturer. HEp-2 cells were seeded into 6-well plates and inhibitors added as described. Cells were washed once in ice-cold Hepes-buffered MEM, before incubation on ice with ^{125}I-Shiga

B sulf-2 (5×10^6 cpm/mL) in the same medium for 20 min. Cells were washed three times with ice-cold PBS and extracted twice with 5% TCA for 5 min. The precipitate was dissolved in 0.1 M KOH and the radioactivity measured on an LKB Wallac 1261 Multigamma γ-counter (Pfizer).

Shiga toxin uptake

Shiga toxin uptake was measured essentially as described previously (25). Shiga toxin-SS-Biotin was prepared by biotinylating Shiga toxin with the reducible EZ-Link Sulfo-NHS-SS-Biotin (Pierce Biotechnology) according to protocol provided by manufacturer. Monoclonal anti-Shiga like toxin 1 antibody (3C10, Toxin technology, Sarasota, FL, USA) was labeled according to manufacturer's descriptions, with BV-TAG-label containing a tris (bipyridine)-chelated ruthenium (II) atom (BioVeris Corporation, Gaithersburg, MD, USA). HEp-2 cells were seeded into 24-well plates and inhibitors added as described. The cells were washed once with Hepes-buffered MEM before incubation with Shiga toxin-SS-Biotin (50 ng/mL) in the same medium for 10 or 45 min. After a brief wash with ice-cold buffer (0.14 M NaCl, 2 mM $CaCl_2$, 20 mM Hepes, pH 8.6), half of the wells were incubated with 0.1 M MESNa in the same buffer supplemented with 2 mg/mL BSA, whereas the other half was mock-treated, for 30 min on ice. Cells were washed once in ice-cold buffer (0.14 M NaCl, 2 mM $CaCl_2$, 20 mM Hepes, pH 7.0) and lysed in lysis buffer (100 mM NaCl, 5 mM $MgCl_2$, 50 mM Hepes, 1% Triton X-100, 60 mM n-octyl β-D-glucopyranoside). Shiga toxin-SS-Biotin was fished out from cell lysates and labeled by gentle shaking with 0.1 mg/mL streptavidin-coated magnetic beads (Invitrogen) and 0.5 μg/mL BV-TAG-labeled anti-Shiga like toxin 1 antibody in assay diluent (0.2% BSA, 0.5% Tween-20 in PBS) for 1.5 h. Electrochemiluminescence from BV-TAG-labeled Shiga toxin-SS-Biotin captured was detected and quantified on a M1R Analyzer (BioVeris Corporation). Counts from MESNa-treated cells correspond to internalized toxin, whereas counts from mock-treated cells correspond to the total amount of toxin associated with the cells.

Sulfation experiments

HEp-2 cells were grown in 6-well plates and inhibitors added as described. Ricin A sulf-1, ricin A-chain modified to contain a tyrosine sulfation site, was produced, purified and reconstituted with ricin B-chain to form ricin sulf-1, as previously described (52). Shiga B sulf-2, Shiga B containing a tandem of sulfation sites in the C-terminus, was produced in *Escherichia coli* BL21(DE3) as previously described (9). The cells were washed twice with sulfate-free medium (MEM 12–126; Bio Whittaker, Verviers, Belgium) supplemented with 1× non-essential amino acids (Bio Whittaker) and 2 mM L-glutamine (Invitrogen) before incubation with the same medium containing 0.2 mCi/mL $Na_2^{35}SO_4$ at 37°C with 5% CO_2. After 3 h, ricin sulf-1 or Shiga B sulf-2 was added to a final concentration of 2 μg/mL, and incubation was continued for 2 h (ricin sulf-1) or 45 min (Shiga B sulf-2). Cell surface-bound ricin sulf-1 was removed by washing the cells with 0.1 M lactose in Hepes-buffered MEM (37°C) followed by 5 min incubation at 37°C with the same medium. The cells were given one brief wash with ice-cold PBS before lysis in lysis buffer (0.1 M NaCl, 10 mM Na_2HPO_4 (pH 7.4), 1mM EDTA, 1% Triton X-100 and 60 mM n-octyl β-D-glucopyranoside) supplemented with protease inhibitors. Cell debris were removed by 10 min centrifugation at 5000 rpm at 4°C, and the recombinant toxins were immunoprecipitated from the cleared lysates overnight at 4°C, with appropriate antibodies immobilized on protein A-Sepharose beads. The beads were washed twice with PBS containing 0.35% Triton X-100, and immunoprecipitated protein was separated by reducing sodium dodecyl sulfate polyacrylamide gel electrophoresis (SDS-PAGE) (12% gel for ricin sulf-1; 4–20% gradient gel for Shiga B sulf-2) and transferred onto PVDF membrane by wet electroblot transfer. Membranes were analyzed by autoradiography. The relative intensities of the bands representing sulfated ricin A sulf-1 (32 kDa) or Shiga B sulf-2 (7.5++ kDa) were estimated using Image Quant Version 5.0 computer software (GE Healthcare) or QuantifyOne 1-D Analysis Software (BioRad), respectively. Total protein sulfation was determined by measuring the ^{35}S content in 5% TCA-precipitated proteins from the lysates immunoprecipitated for ricin sulf-1, using a Packard Tri-Carb Liquid Scintillation Analyzer 2100TR β-counter (PerkinElmer).

Measurement of Shiga toxin cytotoxicity

HEp-2 cells were seeded into 24-well plates and inhibitors added as described. The cells were washed once with leucine-free Hepes-buffered MEM (37°C), and incubated with the same medium for 20 min at 37°C. Increasing concentrations of Shiga toxin were added to the medium, and the cells were further incubated in the presence of toxin for 2 h at 37°C. The cells were washed once with leucine-free Hepes-buffered MEM and incubated with the same medium containing 4 μCi/mL [^{3}H]leucine for 20 min at 37°C. The cells were extracted twice with 5% TCA for 5 min. The precipitate was dissolved in 0.1 M KOH and the radioactivity measured using a Packard Tri-Carb Liquid Scintillation Analyzer 2100TR β-counter (PerkinElmer). Although the deviations between triplicates in such an experiment is low (<10%), and the protection obtained with inhibitors is constant, the toxin concentration required to get 50% inhibition may vary somewhat between different experiments. One representative experiment is therefore presented.

Immunofluorescense confocal microscopy

HEp-2 cells were grown on 8 mm round glass coverslips (Glaswarenfabrik Karl Hecht, Sondheim, Germany) and treated with inhibitors as described. Cells were washed once with Hepes-buffered MEM (37°C) before incubation with Shiga toxin (2 μg/mL) in the same medium for 45 min at 37°C. Cells were washed once with PBS, fixed in formalin solution (Sigma Chemical) for 20 min at room temperature and washed three times with PBS. Cells were permeabilized by incubation with 0.2% Triton X-100 in PBS for 10 min, and washed thereafter three times with PBS. After incubation in block solution (5% fetal calf serum in PBS) for 30 min, cells were incubated with primary antibodies diluted in block solution, for 1 h at room temperature. Then, cells were washed three times for 5 min with block solution before incubation with the appropriate secondary antibodies diluted in block solution for 1 h at room temperature. Coverslips were mounted in mowiol and dried at 37°C. Images were acquired using the laser scanning microscope (LSM) 510 Meta from Carl Zeiss (Oberkochen, Germany).

Annotation of lipid species

MS analyses were performed for species of the following lipid classes: Cer (ceramide), HexCer (hexosylceramide), LacCer (lactosylceramide), TriHexCer (trihexosylceramide, i.e. Gb3), SM (sphingomyelin), PC (phosphatidylcholine), PC-O (PC containing ether bonds, i.e. plasmanyl or plasmenyl PC; plasmenyls often referred to as plasmalogens), PE (phosphatidylethanolamine), PE-O (PE containing ether bonds). It should be noted that the lipid species are listed in the tables and figures in the form of HexCer [42:2] (i.e. showing the total number of carbon atoms and double bonds). As the discussion in the literature about intracellular transport of glycosphingolipids is focusing upon the fatty acid component we have also chosen to do that in our discussion. Thus, the [42:2] species for Cer, SM and all glycosphingolipids are discussed as the lipid species containing the fatty acid 24:1; similarly the [34:1] species are discussed as the species containing the fatty acid 16:0.

MS analyses

Lipids were recovered by a two-step methanol/chloroform extraction as described (53). Settings that ensure accurate and robust quantification have been established in our previous work regarding sample amount, extraction procedure and mass spectrometric measurements (34,53,54). Basically, 900 000 cells (harvested following 4, 24 and 48 h of incubation) were taken up in 180 μL of 155 mM ammonia carbonate and 100 pmol of each lipid standard was added (PE-O 20:0/-O 20:0; PC-O 18:0/-O18:0; SM 35:1; Cer 35:1; GlcCer 30:1) and then extracted with 900 μL chloroform/methanol (10:1), while the water phase was further extracted with chloroform/methanol (2:1). Ceramides, hexosylceramides and lactosylceramides were partitioned into the phase with 10:1 choloroform/methanol content, while other lipids, including Gb3, were enriched in the 2:1 phase. The extracts were dissolved in chloroform/methanol/2-propanol 1/2/4 (v/v/v) containing 7.5 mM ammonium acetate. Before the MS analysis, samples were

vortexed thoroughly and centrifuged for 2 min at 14 000 rpm on a Minispin centrifuge (Eppendorf, Hamburg, Germany). Samples were then loaded onto 96 well plates and sealed with aluminum foil. The lipids were analyzed by MS as described (34) using a LTQ Orbitrap (Thermo Fisher Scientific, Bremen, Germany) instrument equipped with a robotic nanoflow ion source NanoMate HD (Advion BioSciences Ltd, Ithaca, NJ) with 4.1 μm nozzle diameter chip NanoMate HD controlled by Chipsoft 6.4. software (Advion Biosciences) and operated at the ionization voltage of 0.95 kV and gas pressure 1.25 psi in positive ion mode or −1.05 kV in negative ion mode. MS survey scans were acquired using the Orbitrap analyzer operated under the target mass resolution of 100 000 [full width at half maximum (FWHM), defined at m/z 400]. MS/MS experiments on a LTQ Orbitrap instrument were performed using collision-induced dissociation in the linear ion trap or, where specified, in the intermediate C-trap (termed CID and HCD, respectively). Precursors were selected within the m/z window of 1.5 amu (precursor $m/z \pm 0.75$ amu). Acquired MS and MS/MS spectra were interpreted using proprietary software, which identified and quantified the lipid species (Herzog et al., 56th ASMS Conference on Mass Spectrometry 2008). In the 10:1 extracts, the PC, PE and SM species were quantified using the standards for their own lipid classes (described earlier), whereas the relative amounts ('abundance') of Gb3 species (no standard available) were obtained by using the sum of the intensities for the standards of PC, PE and SM. In the 2:1 extracts, Cer and HexCer species were quantified by using the standards for their own lipid classes, whereas the abundance of LacCer (no standard available) was obtained by using the HexCer standard. Thus, as no standards were available for Gb3 and LacCer, we had to show 'abundance,' obtained as described here, whereas other species are reported as pmol per 10^6 cells. The data are reported as mean ± SD based on analysis of three cell extracts analyzed in duplicates ($n = 6$). Subsequent principal component analysis and t-test analysis were performed by MarkerView software (MDS Sciex, Concord, Canada).

Acknowledgments

We are grateful to Anne-Grethe Myrann and Anne Engen for expert technical assistance. The work was supported by The Norwegian Cancer Society, The Norwegian Research Council for Science and the Humanities, The National Programme for Research in Functional Genomics in Norway (FUGE) in the Research Council in Norway.

Supporting Information

Additional Supporting Information may be found in the online version of this article:

Figure S1: Depletion of sphingolipids of HEp2 cells upon incubation with PDMP and FB1. Absolute quantification of sphingomyelin (left column) and LacCer (right column) in HEp2 cells are shown after treatment with 1 μM PDMP (blue squares), 10 μM FB1 (red triangle) and for control cells (black rhombus). Absolute quantities for total class (top row), species with N-linked fatty acid 24:1 (middle row) and species with N-linked fatty acid 16:0 (bottom row) are displayed. Data for the 16:0 species of LacCer are shown in Table S2, but the standard deviation of these data were so large that they are not shown in this figure.

Table S1: Relative abundances of molecular species within sphingolipid classes under control condition and treatment with PDMP and FB1

Table S2: Quantities of monitored glycosphingolipids

Please note: Wiley-Blackwell are not responsible for the content or functionality of any supporting materials supplied by the authors. Any queries (other than missing material) should be directed to the corresponding author for the article.

References

1. Sandvig K, Garred Ø, Prydz K, Kozlov JV, Hansen SH, van Deurs B. Retrograde transport of endocytosed Shiga toxin to the endoplasmic reticulum. Nature 1992;358:510–511.
2. Endo Y, Tsurugi K, Yutsudo T, Takeda Y, Ogasawara T, Igarashi K. Site of action of Vero toxin (VT2) from *Escherichia coli* 0157:H7 and of Shiga toxin on eukaryotic ribosomes. RNA glycosidase activity of the toxins. Eur J Biochem 1988;171:45–50.
3. Ling H, Boodhoo A, Hazes B, Cummings MD, Armstrong GD, Brunton JL, Read RJ. Structure of the shiga-like toxin I B-pentamer complexed with an analogue of its receptor Gb3. Biochemistry 1998;37:1777–1788.
4. Pudymaitis A, Armstrong G, Lingwood CA. Verotoxin-resistant cell clones are deficient in the glycolipid globotriosylceramide: differential basis of phenotype. Arch Biochem Biophys 1991;286:448–452.
5. Sandvig K, Ryd M, Garred Ø, Schweda E, Holm PK, van Deurs B. Retrograde transport from the Golgi complex to the ER of both Shiga toxin and the nontoxic Shiga B-fragment is regulated by butyric acid and cAMP. J Cell Biol 1994;126:53–64.
6. Falguieres T, Romer W, Amessou M, Afonso C, Wolf C, Tabet JC, Lamaze C, Johannes L. Functionally different pools of Shiga toxin receptor, globotriaosyl ceramide, in HeLa cells. FEBS J 2006;273:5205–5218.
7. Römer W, Berland L, Chambon V, Gaus K, Windschiegl B, Tenza D, Aly MR, Fraisier V, Florent JC, Perrais D, Lamaze C, Raposo G, Steinem C, Sens P, Bassereau P, Johannes L. Shiga toxin induces tubular membrane invaginations for its uptake into cells. Nature 2007;450:670–675.
8. Sandvig K, Olsnes S, Brown JE, Petersen OW, van Deurs B. Endocytosis from coated pits of Shiga toxin: a glycolipid-binding protein from Shigella dysenteriae 1. J Cell Biol 1989;108:1331–1343.
9. Lauvrak SU, Torgersen ML, Sandvig K. Efficient endosome-to-Golgi transport of Shiga toxin is dependent on dynamin and clathrin. J Cell Sci 2004;117:2321–2331.
10. Torgersen ML, Lauvrak SU, Sandvig K. Shiga toxin A-chain stimulates clathrin-dependent uptake of the toxin. FEBS J 2005;272:4103–4113.
11. Fujinaga Y, Wolf AA, Rodighiero C, Wheeler H, Tsai B, Allen L, Jobling MG, Rapoport T, Holmes RK, Lencer WI. Gangliosides that associate with lipid rafts mediate transport of cholera and related toxins from the plasma membrane to endoplasmic reticulm. Mol Biol Cell 2003;14:4783–4793.
12. Falguieres T, Mallard F, Baron C, Hanau D, Lingwood C, Goud B, Salamero J, Johannes L. Targeting of shiga toxin b-subunit to retrograde transport route in association with detergent-resistant membranes. Mol Biol Cell 2001;12:2453–2468.
13. Sandvig K, van Deurs B. Membrane traffic exploited by protein toxins. Ann Rev Cell Dev Biol 2002;18:1–14.
14. Sandvig K, van Deurs B. Delivery into cells: lessons learned from plant and bacterial toxins. Gene Ther 2005;12:865–872.
15. Saint-Pol A, Yelamos B, Amessou M, Mills IG, Dugast M, Tenza D, Schu P, Antony C, McMahon HT, Lamaze C, Johannes L. Clathrin adaptor epsinR is required for retrograde sorting on early endosomal membranes. Dev Cell 2004;6:525–538.
16. Del NE, Miserey-Lenkei S, Falguieres T, Nizak C, Johannes L, Perez F, Goud B. Rab6A and Rab6A' GTPases play non-overlapping roles in membrane trafficking. Traffic 2006;7:394–407.
17. Yoshino A, Setty SR, Poynton C, Whiteman EL, Saint-Pol A, Burd CG, Johannes L, Holzbaur EL, Koval M, McCaffery JM, Marks MS. tGolgin-1 (p230, golgin-245) modulates Shiga-toxin transport to the Golgi and Golgi motility towards the microtubule-organizing centre. J Cell Sci 2005;118:2279–2293.
18. Lu L, Tai G, Hong W. Autoantigen Golgin-97, an effector of Arl1 GTPase, participates in traffic from the endosome to the trans-Golgi network. Mol Biol Cell 2004;15:4426–4443.

19. Amessou M, Fradagrada A, Falguieres T, Lord JM, Smith DC, Roberts LM, Lamaze C, Johannes L. Syntaxin 16 and syntaxin 5 are required for efficient retrograde transport of several exogenous and endogenous cargo proteins. J Cell Sci 2007;120:1457–1468.
20. Tai G, Lu L, Wang TL, Tang BL, Goud B, Johannes L, Hong W. Participation of the syntaxin 5/Ykt6/GS28/GS15 SNARE complex in transport from the early/recycling endosome to the TGN. Mol Biol Cell 2004;15:4011–4022.
21. Bujny MV, Popoff V, Johannes L, Cullen PJ. The retromer component sorting nexin-1 is required for efficient retrograde transport of Shiga toxin from early endosome to the trans Golgi network. J Cell Sci 2007;120:2010–2021.
22. Utskarpen A, Slagsvold HH, Dyve AB, Skanland SS, Sandvig K. SNX1 and SNX2 mediate retrograde transport of Shiga toxin. Biochem Biophys Res Comm 2007;358:566–570.
23. Popoff V, Mardones GA, Tenza D, Rojas R, Lamaze C, Bonifacino JS, Raposo G, Johannes L. The retromer complex and clathrin define an early endosomal retrograde exit site. J Cell Sci 2007;120:2022–2031.
24. Walchli S, Skanland SS, Gregers TF, Lauvrak SU, Torgersen ML, Ying M, Kuroda S, Maturana A, Sandvig K. The Mitogen-activated protein kinase p38 links Shiga toxin-dependent signaling and trafficking. Mol Biol Cell 2008;19:95–104.
25. Torgersen ML, Walchli S, Grimmer S, Skanland SS, Sandvig K. PKCdelta is activated by Shiga toxin and regulates its transport. J Biol Chem 2007;282:16317–16328.
26. Arab S, Lingwood CA. Intracellular targeting of the endoplasmic reticulum/nuclear envelope by retrograde transport may determine cell hypersensitivity to verotoxin via globotriaosyl ceramide fatty acid isoform traffic. J Cell Physiol 1998;177:646–660.
27. Sandvig K, Garred O, van Helvoort A, van Meer G, van Deurs B. Importance of glycolipid synthesis for butyric acid-induced sensitization to Shiga toxin and intracellular sorting of toxin in A431 cells. Mol Biol Cell 1996;7:1391–1404.
28. Smith DC, Sillence DJ, Falguieres T, Jarvis RM, Johannes L, Lord JM, Platt FM, Roberts LM. The association of Shiga-like toxin with detergent-resistant membranes is modulated by glucosylceramide and is an essential requirement in the endoplasmic reticulum for a cytotoxic effect. Mol Biol Cell 2006;17:1375–1387.
29. Skanland SS, Walchli S, Sandvig K. Beta-arrestins attenuate p38 mediated endosome to Golgi transport. Cell Microbiol 2009;11:796–807.
30. Hoey DE, Sharp L, Currie C, Lingwood CA, Gally DL, Smith DG. Verotoxin 1 binding to intestinal crypt epithelial cells results in localization to lysosomes and abrogation of toxicity. Cell Microbiol 2003;5:85–97.
31. Perez-Victoria FJ, Mardones GA, Bonifacino JS. Requirement of the human GARP complex for mannose 6-phosphate-receptor-dependent sorting of cathepsin D to lysosomes. Mol Biol Cell 2008; 19:2350–2362.
32. Naslavsky N, McKenzie J, tan-Bonnet N, Sheff D, Caplan S. EHD3 regulates early-endosome-to-Golgi transport and preserves Golgi morphology. J Cell Sci 2009;122:389–400.
33. Garred Ø, van Deurs B, Sandvig K. Furin-induced cleavage and activation of Shiga toxin. J Biol Chem 1995;270:10817–10821.
34. Schwudke D, Hannich JT, Surendranath V, Grimard V, Moehring T, Burton L, Kurzchalia T, Shevchenko A. Top-down lipidomic screens by multivariate analysis of high-resolution survey mass spectra. Anal Chem 2007;79:4083–4093.
35. Kolter T, Sandhoff K. Principles of lysosomal membrane digestion: stimulation of sphingolipid degradation by sphingolipid activator proteins and anionic lysosomal lipids. Annu Rev Cell Dev Biol 2005;21:81–103.
36. Arab S, Lingwood CA. Influence of phospholipid chain length on verotoxin/globotriaosyl ceramide binding in model membranes: comparison of a supported bilayer film and liposomes. Glycoconj J 1996;13:159–166.
37. Shu L, Lee L, Chang Y, Holzman LB, Edwards CA, Shelden E, Shayman JA. Caveolar structure and protein sorting are maintained in NIH 3T3 cells independent of glycosphingolipid depletion. Arch Biochem Biophys 2000;373:83–90.
38. Grimmer S, Iversen TG, van Deurs B, Sandvig K. Endosome to Golgi transport of ricin is regulated by cholesterol. Mol Biol Cell 2000;11:4205–4216.
39. Lieu ZZ, Derby MC, Teasdale RD, Hart C, Gunn P, Gleeson PA. The golgin GCC88 is required for efficient retrograde transport of cargo from the early endosomes to the trans-Golgi network. Mol Biol Cell 2007;18:4979–4991.
40. Sonnino S, Prinetti A, Nakayama H, Yangida M, Ogawa H, Iwabuchi K. Role of very long fatty acid-containing glycosphingolipids in membrane organization and cell signaling: the model of lactosylceramide in neutrophils. Glycoconj J in press.
41. Bonifacino JS, Rojas R. Retrograde transport from endosomes to the trans-Golgi network. Nat Rev Mol Cell Biol 2006;7:568–579.
42. Mukherjee S, Soe TT, Maxfield FR. Endocytic sorting of lipid analogues differing solely in the chemistry of their hydrophobic tails. J Cell Biol 1999;144:1271–1284.
43. Koivusalo M, Jansen M, Somerharju P, Ikonen E. Endocytic trafficking of sphingomyelin depends on its acyl chain length. Mol Biol Cell 2007;18:5113–5123.
44. Sillence DJ, Puri V, Marks DL, Butters TD, Dwek RA, Pagano RE, Platt FM. Glucosylceramide modulates membrane traffic along the endocytic pathway. J Lipid Res 2002;43:1837–1845.
45. Merrill AH Jr, Sullards MC, Wang E, Voss KA, Riley RT. Sphingolipid metabolism: roles in signal transduction and disruption by fumonisins. Environ Health Perspect 2001;109(Suppl. 2):283–289.
46. Smith ER, Merrill AH, Jr. Differential roles of de novo sphingolipid biosynthesis and turnover in the ''burst'' of free sphingosine and sphinganine, and their 1-phosphates and N-acyl-derivatives, that occurs upon changing the medium of cells in culture. J Biol Chem 1995;270:18749–18758.
47. Tam P, Mahfoud R, Nutikka A, Khine AA, Binnington B, Paroutis P, Lingwood C. Differential intracellular transport and binding of verotoxin 1 and verotoxin 2 to globotriaosylceramide-containing lipid assemblies. J Cell Physiol 2008;216:750–763.
48. Johannes L, Tenza D, Antony C, Goud B. Retrograde transport of KDEL-bearing B-fragment of Shiga toxin. J Biol Chem 1997;272:19554–19561.
49. Girod A, Storrie B, Simpson JC, Johannes L, Goud B, Roberts LM, Lord JM, Nilsson T, Pepperkok R. Evidence for a COP-I-independent transport route from the Golgi complex to the endoplasmic reticulum. Nature Cell Biol 1999;1:423–430.
50. White J, Johannes L, Mallard F, Girod A, Grill S, Reinsch S, Keller P, Tzschaschel B, Echard A, Goud B, Stelzer HK. Rab6 coordinates a novel Golgi to ER retrograde transport pathway in live cells. J Cell Biol 1999;147:743–760.
51. Pulvirenti T, Giannotta M, Capestrano M, Capitani M, Pisanu A, Polishchuk RS, San PE, Beznoussenko GV, Mironov AA, Turacchio G, Hsu VW, Sallese M, Luini A. A traffic-activated Golgi-based signalling circuit coordinates the secretory pathway. Nat Cell Biol 2008;10:912–922.
52. Rapak A, Falnes PO, Olsnes S. Retrograde transport of mutant ricin to the endoplasmic reticulum with subsequent translocation to cytosol. Proc Natl Acad Sci USA 1997;94:3783–3788.
53. Ejsing CS, Sampaio JL, Surendranath V, Duchoslav E, Ekroos K, Klemm RW, Simons K, Shevchenko A. Global analysis of the yeast lipidome by quantitative shotgun mass spectrometry. Proc Natl Acad Sci USA 2009;106:2136–2141.
54. Grimard V, Massier J, Richter D, Schwudke D, Kalaidzidis Y, Fava E, Hermetter A, Thiele C. siRNA screening reveals JNK2 as an evolutionary conserved regulator of triglyceride homeostasis. J Lipid Res 2008;49:2427–2440.